

Author



Comparing the Evolutionary Significance of Nonlytic and Lytic Viruses Using the Euler-Lotka Equation

Amanda Janesick

Genetics and Mathematics

When she arrived at UCI, Amanda Janesick was delighted to discover the research opportunities available to her so early in her college career. She has loved the experience of working one on one with Professor Komarova, using mathematical modeling to study a variety of biological and evolutionary phenomena from language acquisition to cancer progression. Amanda's research experience has taught her many invaluable lessons, and her interdisciplinary studies have helped her find a unique place within the culture and vitality of the campus. Before beginning her studies at UCI, Amanda spent three years dancing professionally with the Nevada Ballet Theatre in Las Vegas.

Key Terms

- ◆ Euler-Lotka Equation
- ◆ Infectivity
- ◆ Lytic
- ◆ Nonlytic
- ◆ Pathogenesis
- ◆ Viral Proliferation Rate

Abstract

Viral pathogenesis is a growing area of interest in biology, with implications ranging from the suppression of tumor growth to the control of HIV propagation. We investigated the evolution of viral release strategies from a computational biology perspective. Viruses are either lytic (they lyse, or kill, the host cell) or nonlytic (they bud, or leak, from the host progressively). This paper asks which strategy leads to the most rapid spread of viral progeny. The Euler-Lotka equation is our chosen instrument, and its induction into virus dynamics is novel. The model generated with the Euler-Lotka equation incorporates parameters that describe how fast virions accumulate or exit the cells and how the cells respond to a viral infection. Our results show that a nonlytic virus exhibits greater growth rates than a lytic virus, with all parameters equal. Given this outcome, parameters are adjusted to find the conditions that confer an evolutionary advantage to the lytic virus. We conclude that a lytic virus should have low cytotoxicity, possess a short eclipse stage (time delay inherent to the viral life cycle), or breed progeny at relatively high rates.

Faculty Mentor



Viral release strategies can be roughly classified as lytic (which accumulate inside the host cell and exit in a burst, killing the cell), and budding (which are produced and released from the host cell gradually). Amanda Janesick used mathematical modeling to study the evolutionary competition between these two strategies. She employed the Euler-Lotka model, an equation that comes from the mathematical theory of demography, to show exactly the circumstances under which lytic viruses have a chance in a competition against budding viruses. It has been a pleasure to work with Amanda because of her keen interest in the scientific question, inquisitive mind, quick learning, and ability to understand the bigger picture.

Natalia Komarova

School of Physical Sciences

Introduction

Viruses are versatile agents with a multitude of cell-killing strategies. Although the range of cytopathic effects (extent of damage to host cells) varies significantly between strains, there are two main modes of viral release: bursting (lytic) and leaking (nonlytic). A virus is lytic if it ruptures the host cell and releases progeny that infect other cells. A virus is nonlytic if it exits the cell via exocytosis, with progeny budding out of the plasma membrane until host death. There is ongoing biological research on the genetic determinants and molecular mechanism of viral release. Our study of viruses is performed by mathematical modeling, rather than laboratory experiments. We employ the Euler-Lotka equation to simulate the life cycle of viruses and their hosts. A large portion of this paper is devoted to the derivation of the equation and the biological justification of its components. After the model is developed, we discuss the conditions under which nonlytic or lytic viruses are evolutionarily favorable.

Background

Previous Research in Virus Dynamics

Viral pathogenesis is amenable to mathematical modeling and population dynamics. Past work in this field has answered fundamental questions about the relationship between host mortality and virulence (Nowak and May 81). Researchers have discredited the long-standing theory that evolution favors survival of apathogenic viruses (Anderson and May, 1996). Such a faulty assumption is “pleasing to human sensibilities” (Levin 93), because a virus is presumably most efficient when its host remains unharmed. However, viruses have been shown to optimize their growth rate, leading to only moderate levels of pathogenesis (Nowak and May, 1994). Our project differs in both technique (i.e. the debut of the Euler-Lotka equation) and purpose. We specifically investigate the evolution of lytic and nonlytic viral strategies, rather than exploring the preservation of virulence. We address the evolution of viral lifestyle—not pathogenesis—to determine which strategy leads to the most rapid spread of viral progeny.

History of the Euler-Lotka Equation

The Euler-Lotka equation (Equation 1) is most often employed to approximate the growth rate, Γ , of an age-structured or age-specific population.

$$1 = \int_0^{\infty} e^{-\Gamma x} [g(x) F^S(x)] dx \quad (1)$$

Developed independently by Leonhard Euler and Alfred Lotka in the early 1900s (Neal 234), the equation includes such parameters as survivorship, $F^S(x)$, and fecundity, $g(x)$, both varying with respect to a specific age class, x , of the population. Incorporating these parameters gives the Euler-Lotka equation an advantage over the typical logistic model in which growth rate is solely dependent upon population density (Murray 20). When the equation is solved for Γ , the “natural rate of increase” of the population is revealed (Lotka 111). The Euler-Lotka equation assumes that the population maintains a state of long-term dynamic equilibrium. That is, the system is stable and fairly elastic—it will return to normal if perturbed (Lotka 110). Therefore each age class is expected to grow exponentially at the same rate, Γ .

Methods

Euler-Lotka Equation: Application to Virus Dynamics

Suppose that a population of cells is infected by a virus that possesses one of three proliferation strategies: nonlytic, lytic, or a combination of both. The Euler-Lotka equation applied to virus dynamics is actually derived with respect to the combination strategy:

$$1 = \int_0^{\infty} e^{-\Gamma x} \left[\underbrace{F^S(x) \cdot g(x)}_{\text{Nonlytic Term}} + \underbrace{f(x) \cdot r(x)}_{\text{Lytic Term}} \right] dx \quad (2)$$

An attractive quality of Equation 2 is that its nonlytic and lytic elements can be separated, and the combination strategy left intact. The complete derivation of Equation 2 is in Appendix A. Notice that two additional parameters have been incorporated: the lifetime probability distribution of cells, $f(x)$, and the number of virions released upon cell lysis, $r(x)$. The remaining parameters, $F^S(x)$ and $g(x)$, closely resemble their demographic counterparts by representing the survivorship and infectivity (i.e., rate of budding virions) of cells, respectively. The variable x reminds us that the population of cells is still age-structured. By definition, the population includes only infected cells; hence, each age class x is defined by the duration of infection, not by the lifespan of the cell.

Modeling Cell Mortality

An important aspect of Equation 2 is the modeling of cell death. Viruses are only as prolific as their hosts. Cell mortality concerns two related terms: the lifetime probability distribution, $f(x)$, and the survivorship function, $F^S(x)$. For

this experiment, the following exponential distribution is incorporated:

$$f(x) = \frac{\theta(x-\Delta)e^{-\frac{x-\Delta}{\tau-\Delta}}}{\tau-\Delta}; \quad \Delta < \tau \quad (3)$$

Here, τ is the average cell lifespan that is used to quantify the diverse cytopathic effects of viruses. The Heaviside function is given by θ , and its time delay, Δ , represents the period during which *all* cells remain alive. From the moment of viral transmission ($x = 0$) to the beginning of cell fatalities ($x = \Delta$), the lifetime distribution returns a value of zero. Biologically, Δ measures the intensity of cell immune response to an infection. For our purposes, Δ is independent of τ , although one could assume a correlation between the immune response and cytotoxicity of viruses. For simplicity, delaying the death threshold *does not* increase the probability that an average cell will live longer. Because $f(x)$ is normalized to have an average lifespan equal to τ , Δ merely affects the delay and the magnitude of the $f(x)$ downslope (Figure 1a).

There are two special cases to consider when Δ approaches 0 or τ :

$$\text{Special Case I: } \Delta \rightarrow 0 \Rightarrow \lim_{\Delta \rightarrow 0} f(x) = \frac{e^{-\frac{x}{\tau}}}{\tau} \quad (4)$$

$$\text{Special Case II: } \Delta \rightarrow \tau \Rightarrow \lim_{\Delta \rightarrow \tau} f(x) = \delta(x-\tau) \quad (5)$$

In situations where a virus elicits an immediate immune response, Equation 4 becomes more appropriate. Cell mortality is certainly not restricted to physical damage caused by lysing or budding, which require time for viral replication (Carrasco 2). Rather, viruses and their hosts have developed several mechanisms of cell death (including apoptosis), whereby a damaged cell is systematically destroyed. This “abortive” process renders Δ quite short (Cann 192). Researchers have yet to attribute premature death to the host’s need to curtail the spread of viral progeny or to the virus’s desire to hasten the transmission process (Cann 175). Nevertheless, viruses encode “death-promoting proteins,” which bring forth an immune response, often resulting in host mortality well before the assembly of progeny (Abou El Hassan et al., 2004).

Equation 5 reduces Equation 3 to the “Dirac” delta function (offset by τ), which reflects the possibility that cell death is deterministic, or abrupt, rather than gradual. In this case, cells remain alive until $x = \tau$, at which point they all die off rather instantaneously. Case II is best applied to

virulent, lytic viruses, which rarely establish the persistent or latent infections that characterize many nonlytic strains. Infections by viruses such as HIV, that launch a tug-of-war between host cell mortality and viral replication, cause cell death to occur in a stochastic fashion. In contrast, lytic and aggressive strains like the Newcastle disease virus (NDV) induce necrosis, apoptosis, and cell lysis almost simultaneously and with mild predictability (Kommers et al, 2003). Such a scenario is most properly modeled by the “Dirac” delta function.

The lifetime probability distribution, $f(x)$, is naturally associated with the survivorship function, $F^S(x)$. The probability that an infected cell will survive until x is obtained by integrating the probability distribution from an arbitrary x to infinity:

$$F^S(x) = \int_x^{\infty} f(t) dt = 1 + \theta(x-\Delta)e^{-\frac{x-\Delta}{\tau-\Delta}} - \theta(x-\Delta) \quad (6)$$

The lifetime probability distribution, $f(x)$, as well as the resulting survivorship curve, $F^S(x)$, is depicted in Figure 1.

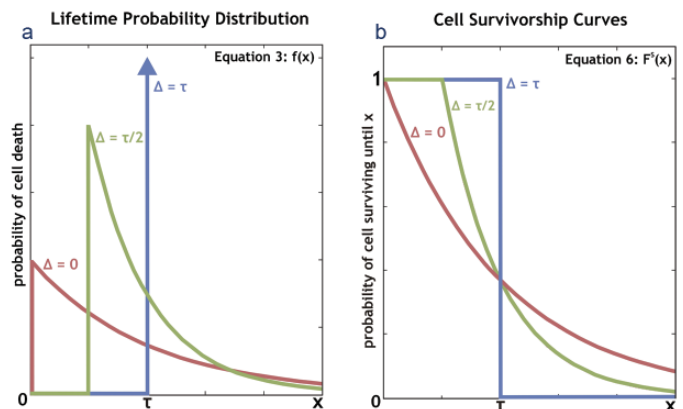


Figure 1

Graphical Demonstration of $f(x)$ and $F^S(x)$. Figure 1a shows the lifetime probability distribution of an infected cell for $\Delta = \tau/2$, $\Delta = 0$ (Case I), and $\Delta = \tau$ (Case II). Figure 1b shows the cell survivorship curves, each representing the probability of surviving until an arbitrary age class, x , for three different values of Δ .

Modeling Cell Infectivity

We assumed that the number of viruses manufactured within infected cells follows a linear law. Most evidence points to linear viral kinetics, although there are indications of exponential production of virions (Yasuda et al. 288, Mangor et al. 2549). Live cells infected by nonlytic viruses have a natural infectivity, budding a constant number of *productive* viruses (those that are able to infect other cells) per second, given by $g_N(x)$, where the subscript “N” denotes “nonlytic.” The rate of accumulation of virions within the host cell is

given by $g_L(x)$, where “L” denotes “lytic.” Integrating $g(x)$ from the beginning of virus assemblage until cell death gives $r(x)$, the virulent capacity or infectivity of lysed cells:

$$\text{Rate of egress (budding): } g_N(x) = c_1 \cdot \theta(x - \lambda) \quad (7)$$

$$\text{Rate of accumulation: } g_L(x) = c_2 \cdot \theta(x - \lambda) \quad (8)$$

$$\text{Capacity of lysed cells: } r(x) = \int_0^x g_L(t) dt = c_2 \cdot (x - \lambda) \quad (9)$$

Here, c_1 and c_2 are the magnitudes of the budding and accumulation rates, respectively. The time delay, λ , has different meanings for nonlytic and lytic viruses. λ_N represents the latent period, the time from infection to the appearance of the first extracellular virus. λ_L symbolizes the eclipse period, the time from infection to the appearance of the first intracellular virus (Mediratta & Essani, 93). For our project, it was assumed that $\lambda_N = \lambda_L$, although we devote a small portion of work to the situation where $\lambda_N \neq \lambda_L$. Unlike Δ , there is no reason to investigate the case where $\lambda = 0$, because a virus without a latent or eclipse period is unlikely. Introduction of λ allows us to quantify the previous discussion regarding cell death induction. When the cell expires before maturation of the viral progeny, we say that $\Delta < \lambda$.

The Functional Euler-Lotka Equation

Our first step was to split Equation 2 into its lytic and nonlytic terms. Then, substituting Equations 3, 6, 7, and 9 into each component of Equation 2 yields Equations 10 and 11:

$$\begin{aligned} \text{Nonlytic: } 1 &= \int_0^\infty e^{-\Gamma x} [F^S(x) \cdot g_N(x)] dx \\ 1 &= c_1 \int_0^\infty \theta(x - \lambda) \cdot e^{-\Gamma x} \left[1 + \theta(x - \Delta) e^{-\frac{x-\Delta}{\tau-\Delta}} - \theta(x - \Delta) \right] dx \quad (10) \end{aligned}$$

$$\begin{aligned} \text{Lytic: } 1 &= \int_0^\infty e^{-\Gamma x} [f(x) \cdot r(x)] dx \\ 1 &= \frac{c_2}{\tau - \Delta} \int_0^\infty (x - \lambda) \cdot e^{-\Gamma x} \left[\theta(x - \Delta) \cdot e^{-\frac{x-\Delta}{\tau-\Delta}} \right] dx \quad (11) \end{aligned}$$

The expressions obtained from solving Equations 10 and 11 are in Appendix B. These are graphed numerically and presented in the Results portion of this paper. However, before presenting the data, a few parameters must be identified.

Table 1

Summary of parameters and their descriptions used in this paper.

Parameter	Description	Parameter	Description
x	age class of cell population	λ	latent/eclipse stage of viral life cycle
τ	average cell lifespan	Δ	severity of immune response
Γ	virus proliferation rate	$g_N(x)$	rate of egress (budding) of virions
$f(x)$	lifetime probability distribution	$g_L(x)$	rate of accumulation of virions
$F^S(x)$	cell survivorship function	$r(x)$	infectivity of lysed cells
θ	Heaviside function	c_1	magnitude of budding rate
δ	“Dirac” delta function	c_2	magnitude of accumulation rate

The Δ - λ Relationship. There is a competition between Δ , the period during which all cells are alive, and λ , the latent or eclipse stage of the virus life cycle. From a biological perspective, two situations are equally viable in either lytic or nonlytic viruses: $\lambda > \Delta$ or $\lambda < \Delta$. The former describes a population of infected cells that begins to die from immune response before viral progeny are produced. The latter describes a population that only begins to suffer fatalities after the progeny is produced.

The Δ - τ Relationship. An assumption with Equation 3 (the lifetime probability distribution) is that τ must be greater than Δ . With all the cells alive throughout Δ , the average cell lifespan cannot fall within this window of time. The $\tau > \Delta$ relation manifests itself clearly in the succeeding graphs. Numerical results are altered such that any Γ falling within the $\tau < \Delta$ region is set to zero and the curves are often truncated, depending on the value of λ .

The Combination Strategy. The right hand sides of Equations 10 and 11 can be added and set equal to 1, resulting in an expression for the unification of both nonlytic and lytic techniques. Because both c_1 and c_2 are included within the combination expression, a virus using both budding and lysing techniques would appear to have a competitive advantage. We presume that this is not the case. That is, the production rates must be scaled such that $c_1 + c_2 = K$, where nonlytic viruses have rate $c_1 = K$, and lytic viruses have rate $c_2 = K$. Evidence for combination strategies in which a virus first diffuses out of the cell and then bursts the remaining progeny is rarely documented. A few researchers

have recorded cases within the family *Reoviridae* in which viral progeny are released only a few hours postinfection, well before cell lysis (Cromack et al., 1971).

Special Cases I and II. As before, two special cases result from taking the limit of Equations 10 and 11 with respect to Δ . Both equations are condensed under these unique circumstances and their expressions are in Appendix B. Case I ($\Delta \rightarrow 0$) requires that λ be greater than Δ , otherwise the viral progeny would be manufactured before the cells are infected. Case II ($\Delta \rightarrow \tau$) calls for λ to be less than τ , otherwise, all the cells would be dead from immune response before the virus has the opportunity to assemble its progeny.

Numerical Analysis

Equations 10 and 11 do not result in explicit expressions; therefore, most subsequent information stems from graphical analysis of Γ . We numerically solved for Γ , the viral proliferation rate, as a function of τ , the average cell lifespan. This task was accomplished with the use of MATLAB® 7.0. From the resulting figures we determined the conditions under which Γ is maximized or minimized.

Results

The main goal of our calculations was to compare the proliferation rates of nonlytic and lytic viruses, as well as investigate two special cases. Recall that Case I ($\Delta \rightarrow 0$) reflects the scenario in which cells elicit an immediate immune response. Case II ($\Delta \rightarrow \tau$) models the instantaneous death of cells reacting to a destructive, highly pathogenic virus. Figure 2 presents a comparison of the nonlytic and lytic strategies under normal conditions as well as for both special cases defined previously. We hold λ , c_1 and c_2 constant to prevent either strategy from receiving an advantage. Notice that the nonlytic virus exhibits greater growth rates: $\Gamma_N > \Gamma_L$ for all τ . This result is especially apparent for large τ where Γ_L asymptotically approaches zero. In contrast, Γ_N reaches a plateau rather than a decline. Indeed, calculation of $\tau \rightarrow \infty$ reveals a carrying capacity solely determined by λ and c_1 : $\Gamma = c_1 e^{-\tau\lambda}$. Even at peak viral proliferation, Γ_L never surpasses Γ_N under equal conditions.

Figure 2 also shows variation in τ -intercepts where $\Gamma = 0$. Either the τ -intercepts are dissimilar or they are nonexistent. The latter can be attributed to the condition where $\Delta > \tau$ and the curves are truncated, with no τ -intercept established. If a τ -intercept does exist, its expression is given by $\tau = (1 + c_1 \lambda) / c_1$, except in nonlytic Case I ($\Delta \rightarrow 0$), which possesses a unique τ -intercept given by a different

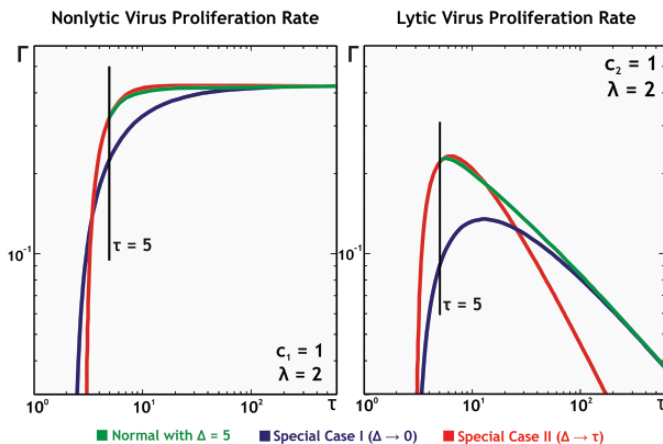


Figure 2

Nonlytic and Lytic Proliferation Rates with General and Special Cases I and II. These two diagrams, in logarithmic scale, project budding and lysing strategies side by side for constant λ , c_1 and c_2 . Equations 10 and 11 depend on an arbitrary $\Delta > 0$, so we choose $\Delta = 5$, and truncate the curves appropriately.

expression ($\Gamma = c_1 \tau e^{-\lambda\tau}$). Another outcome of Figure 2 is the behavior of the lytic Case II curve as $\tau \rightarrow \infty$, which falls to zero much faster than the others.

Figure 3 illustrates how each viral lifestyle is affected by changes in the immune response of the cell, D , or the latent/eclipse period of the viral life cycle, λ . Figure 3 shows that an increase in Δ results in both a decrease and delay in the maximum proliferation rates, especially for lytic

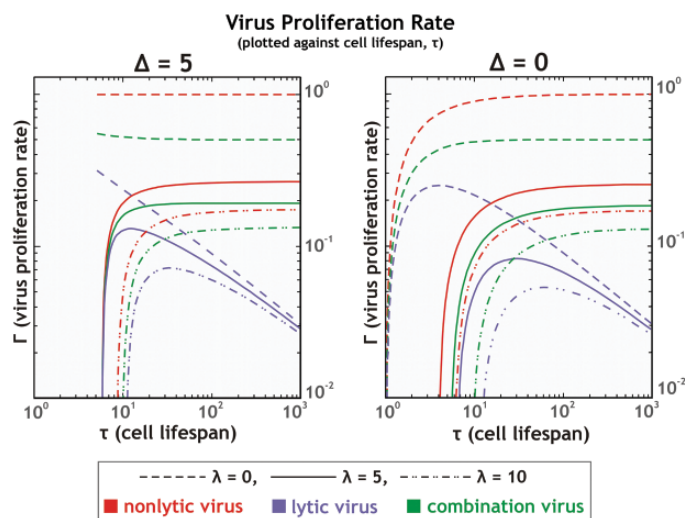


Figure 3

Virus Proliferation Rates with Varying λ and Viral Strategies for Two Values of Δ . The combination production rates are scaled down ($c_1' = 0.5$, $c_2' = 0.5$) to prevent an unfair competitive advantage. Variation in line style is employed to portray three values of λ , strategically selected for investigation of the Δ - λ relationship.

viruses. An increase in λ produces lower proliferation rates and causes a loss of low τ -values.

Discussion

Overall Implications of Graphical Results

Perhaps the most significant outcome of Figures 2 and 3 is that nonlytic viruses exhibit greater growth rates: $\Gamma_N > \Gamma_L$ for all τ . The success of a lytic virus is correlated with cell mortality; hence, a nearly immortal host cell will prohibit the spread of viral progeny. A nonlytic virus infecting the same host would have greater reproductive fitness. For this reason, we see the nonlytic virus proliferation rate reaching a plateau rather than a decline. Even at peak viral proliferation, Γ_L never surpasses Γ_N under equal conditions. Yet many picornaviruses and adenoviruses also lyse their host (Voyles 225). The evolutionary gain from cell lysis is a mystery recognized by few researchers (Carrasco 107). We provide a preliminary solution through the adjustment of certain variables that give a competitive advantage to the lytic virus.

Special Cases I and II

Nonlytic Case I ($\Delta \rightarrow 0$) has a unique τ -intercept at $\Gamma = 0$ (see Figure 2), which is a mathematical artifact allowing viruses to escape early from cells with short lifespans.

$$\text{Nonlytic Special Case I: } 1 = c_1 \tau e^{-\lambda/\tau} \quad (12)$$

$$\text{All Other Cases } (\lambda > \Delta): \tau = (1 + c_2 \lambda)/c_2 \quad (13)$$

τ -intercepts do not exist for $\lambda < \Delta$ due to curve truncation (Figure 2 shows this happening for $\lambda = 2, \Delta = 5$). The end result is a budding virus with the ability to assemble progeny for short cell lifespans. However, Figure 2 reveals that nonlytic Case I produces lower overall rates of proliferation for a wide range of τ values.

Lytic Case II possesses some fascinating properties as well. The manner in which this virus asymptotically falls to zero as $\tau \rightarrow \infty$ is unique (Figure 2). The rate of decline is faster, caused by the location of τ in the exponential, in contrast to the simple τ/τ^2 competition exhibited by all other lytic curves (see Appendix B). Earlier, we proposed that Special Case II suited highly cytotoxic viruses in nature. Figure 2 confirms that viruses able to lyse an entire population of cells function best when the host lifespan is short. As the lifespan grows longer, their efficiency decreases dramatically.

Evolution of the Latent Infection

Limiting our attention to the direct consequences of λ variation, we find 2-dimensional curve shifting (Figure 3). As λ lengthens, the virus proliferation rate deteriorates (vertical shift) and the τ -values required to return even a minimal proliferation rate are increased (horizontal shift). From a biological perspective, a long latent or eclipse period can be caused at various points in the viral replication cycle. In the case of the Measles virus, replication of genetic material and protein synthesis is quick, but maturation of virions is protracted (Portner & Bussell 46). In Simian Virus 40, entry, transit and uncoating is swift, but viral gene expression is slow (Clever et al. 7333). Regardless of how the λ delay is spent, cells that die quickly do not return any proliferation rate because they expire before the viral progeny is synthesized.

The shifting of the curves towards the right with increased λ is fairly intuitive and makes an important evolutionary point. Figure 3 provides evidence that latent infections, like those established by the Herpes virus, are characterized by strong host cell survivorship (Ruf). Viruses that allow their hosts to survive and live long are generally nonlytic. In contrast, lytic viruses deserve no consideration for large τ , even after certain variables are adjusted (see “Giving Lytic Viruses an Evolutionary Advantage,” below).

Now that we have established the connection between long host cell lifespans and nonlytic viruses, we can address the findings that lengthening λ decreases proliferation rate for all τ . Figure 3 provides an argument against the evolutionary advantage of a latent infection for nonlytic viruses. Peak nonlytic proliferation rate ($\Gamma = c_1 e^{-\Gamma\lambda}$) is completely reliant on λ . Γ diminishes as λ lengthens. Therefore, we propose that latent infections have evolved not due to propagation efficiency, but for other reasons. For instance, suppose that viruses establish latent infections such that they can “wait” for the right environmental conditions to release progeny.

Δ -Sensitivity

Curve truncation is one effect of Δ variation, but let us now focus on Δ -sensitivity. That is, the curvature and local maxima of Figure 3 change when Δ is altered. Since none of the limiting expressions depend on Δ , these transformations are not easy to quantify. The lytic virus has greater Δ -sensitivity than its nonlytic counterpart, although the effects are similar. Viewing the lytic curves alone for constant λ, c_1 and c_2 , we witness both a decrease and delay in maximum proliferation potential for lytic viruses. The nonlytic curves tend to reach their maximum later; however, the final plateau remains unchanged. These changes in curve structure

occur because an immediate immune response (small Δ) requires that the cell population live longer, on average, for the virus to yield maximum proliferation rates. Of course these rates can never surpass those obtained by viruses that pass the immune system undetected. A population of cells infected by such a virus results in larger Δ , allowing the virus to take advantage of the entire cell population.

Giving Lytic Viruses an Evolutionary Advantage

All parameters being equal, we have discovered that $\Gamma_N > \Gamma_L$ for all τ . This means we must unearth the techniques that lytic viruses have acquired to survive throughout the evolutionary process. Earlier discussions have deduced certain conditions that maximized viral proliferation rate. By altering variables like λ , τ , c_1 , and c_2 , we can begin to theorize how lytic viruses may have evolved. Nonlytic and lytic viruses behave differently in nature; hence, assumptions like equal production rates ($c_1 = c_2$) or equal latent/eclipse periods ($\lambda_N = \lambda_L$) are unfair. Therefore, we focus on making the lytic virus evolutionarily advantageous for relatively short τ .

The τ Lytic Advantage

For all parameters being equal, we discover that there exists a range of lytic τ values (τ_L) such that $\Gamma_L > \Gamma_N$ for certain nonlytic τ values (τ_N). The τ lytic advantage occurs under relative, not exact circumstances, although two conditions are required: Δ must be less than λ , and the lytic virus must have lower cytotoxicity, $\tau_L > \tau_N$ (the host cell infected by lytic viruses has a longer lifespan). Figure 4a demonstrates this effect. Of course experimental evidence does not support the tendency of lytic viruses to be less cytopathic. For example, ebola is a destructive, cytotoxic virus and its mechanism of release is cell lysis, not budding (Baize et al., 2000). Hence, we conclude that variation in other parameters must be at work. Indeed, changing λ , Δ , c_1 , and c_2 in lytic versus nonlytic viruses alters the logic of the τ advantage significantly. That is, we begin to find that the reverse is true: lytic viruses become more cytopathic to gain an advantage.

The λ Lytic Advantage

We now consider the scenario where $\lambda_L \neq \lambda_N$, and truly distinguish between the nonlytic latent period (time until extracellular appearance of virions) and the lytic eclipse period (time until intracellular appearance of virions). The eclipse period always occurs sooner because accumulating virions within the cell is quicker than extrusion of virions through the plasma membrane (Cann 106). In addition, lytic viruses are generally naked in structure, consisting entirely of

genetic material and protein. Most nonlytic viruses require the synthesis of lipids and glycoproteins to build extensive envelopes (Cann 40). The simplicity of lytic structure allows progeny to be assembled faster; hence, we can safely assume $\lambda_L < \lambda_N$.

Figure 4b demonstrates the λ lytic advantage by comparing three values of λ_L to a fixed and larger λ_N curve. In addition, Figure 4b identifies three points along the nonlytic curve for discussing which values of τ_L promote the greatest benefit. As an example, suppose that a nonlytic virus has a lifespan given by Point 1. Comparing all three λ_L curves to the Γ_N obtained at Point 1, we find that there always exists some τ_L such that $\Gamma_N < \Gamma_L$. As λ_L increases and approaches λ_N the restriction $\tau_L > \tau_N$ must hold (exemplified for $\lambda_L \geq 5$ in Figure 4b). Points 2 and 3 can be analyzed similarly. Notice at Point 3, only $\lambda_L = 1$ has the ability to compete with the nonlytic curve, and achieves a proliferation rate superior to Γ_N for any τ_N value.

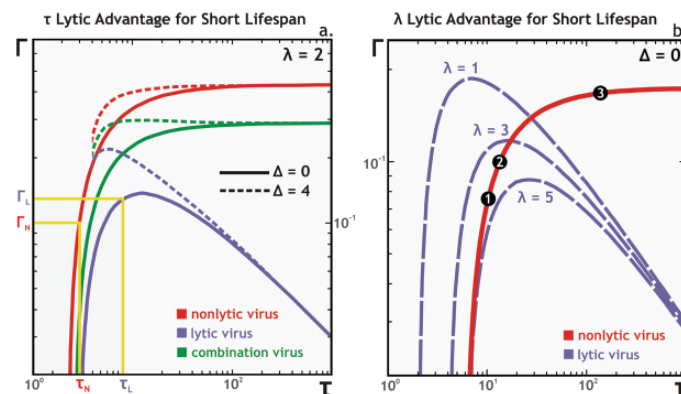


Figure 4
 τ and λ Lytic Advantages Compared to a Nonlytic Competitor. Figure 4a illuminates arbitrary values of τ_N and τ_L whereby $\Gamma_L > \Gamma_N$. The dotted lines demonstrate the case where $\Delta > \lambda$, such that the lytic advantage cannot be conferred. Figure 4b shows three different λ_L values each to be compared with three points along the λ_N curve.

The c_2 Lytic Advantage

Adjusting the values of c_1 and c_2 shifts all curves vertically. For the same reason we assumed that lytic viruses have short λ , we also propose that lytic viruses produce progeny at a faster rate. This occurs because accumulating viruses within the cell is physically easier than budding. While adjusting c_1 and c_2 , we can also take another look at the combination virus. We assume that the combination virus accrues progeny at a certain rate and leaves the cell spontaneously at a different rate. Figure 5 demonstrates the c_2 lytic advantage. Also, addressing τ values we find that $\tau_L > \tau_N$ when $c_1 = c_2$. As mentioned above, the observation that lytic viruses are

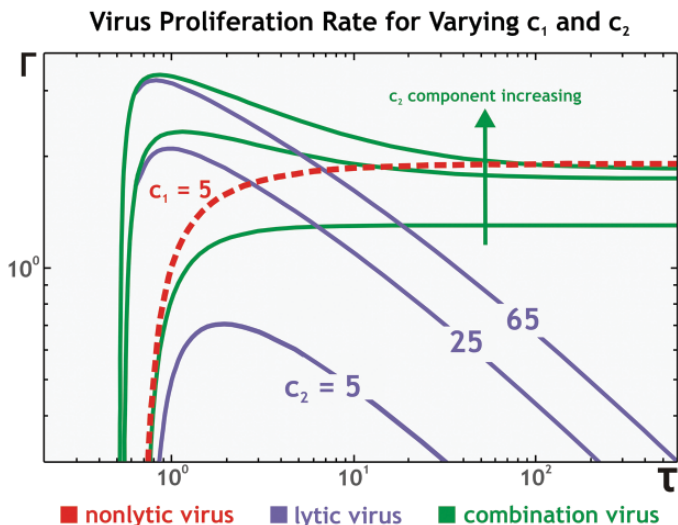


Figure 5

The c_2 Lytic Advantage Compared to a Fixed Nonlytic Competitor. All variables are held constant except c_2 , which is adjusted until $\Gamma_L > \Gamma_N$ for short τ . The c_1 and c_2 values are not additive in the combination virus. Rather, the relationship between c_1 and c_2 has been scaled to reflect a general increase in the c_2 component.

required to be less cytopathic is not realistic. Hence, we conclude that $c_1 < c_2$ because it places the greatest lytic proliferation rate where $\tau_L < \tau_N$.

Conclusion

The mission of this project was to explore evolutionary pressures acting on lytic and nonlytic viruses, using the proliferation rate (Γ) as a measure of fitness. The Euler-Lotka equation creates a reasonable modeling base, yielding valuable graphical results. Originally, we found that a nonlytic virus exhibits greater proliferation rates than a lytic virus and that a lytic virus only attains an advantage when it is less cytopathic (large τ_L). Since this is improbable (lytic infections are generally more cytotoxic), parameters like λ_L and c_2 were adjusted to give the lytic virus an advantage. Reducing λ_L and increasing c_2 were realistic modifications, imparting the less complex structure of the lytic virus to the model. Thus, shortening the eclipse stage, lowering the cytotoxicity, and amplifying viral accumulation rates conferred an evolutionary advantage to the lytic virus.

In addition to findings that satisfied the main hypothesis, other interesting results were uncovered. Investigation of the latent period of a nonlytic virus (λ_N) confirmed the biological reality that latent infections are characterized by strong host cell survivorship. Moreover, we found that a latent infection evolves for reasons other than high proliferation rates (e.g., ability for the virus to wait for proper envi-

ronmental conditions). Analysis of Δ -sensitivity revealed that a virus eliciting a strong immune response from the host should be less cytopathic. This implies that a virus can afford to be more toxic to its host cell if the host's immune system cannot detect it.

Future work will expand the model to include more biological details. For example, we will have the immune system play a more dynamic role in the prevention of virus proliferation. Above, the time delay, Δ , was used to represent the speed of the host's immune response to an infection. This affected the shapes of the cell lifespan distribution and the survivorship curve. Our new model will be constructed such that the immune system detracts from the rate of accumulation and exit of virions. Instead of the cells' releasing a fixed number of viruses, antibodies will kill the viruses at a specific rate. Our hypothesis is that the lytic virus will hold the advantage in this situation. A bursting cell can produce a large amount of progeny in a short time interval, perhaps dodging the full strength of the immune system.

Computational biology is an emerging, vastly interdisciplinary field of research. Using mathematics to model intricate, nonlinear biological systems serves to interpret diverse phenomena in nature. Combined with advancements in computer technology, the field provides insight and solidity to modern biological theories. Research in virus dynamics holds great potential, especially in the development of antiviral drugs. This area of medical science has a history of inefficiency with the overuse of trial and error methods. The advent of DNA sequencing has improved the effectiveness of preventative vaccines significantly. However, due to the complexities of genetic analysis, antiviral research can benefit from the clarity of a modeling approach. We expect our results to provide information that can help others produce drugs to reduce viral proliferation rates in either lytic or nonlytic infections.

Appendix A: Derivation of the Euler-Lotka Equation

Suppose that a population of cells is infected by a virus at time t . We will only give credence to viruses that actually manage to infect other cells. Let $V(t)$ = the number of *productive* viruses released by the cells. The population of infected cells is age-structured, and each age class, x , is defined by the duration of infection. In general, live cells release a certain amount of virions (via budding), while dying cells release a different amount (via lysing) upon death. The number of viruses released from live cells at time t is the product of $A(x, t)$, the number of cells alive

within a specific age class, and $g(x)$, the rate of egress of virions, summed over all age classes:

$$V_N(t) = \sum_{x=0} A(x,t) \cdot g(x) \quad (\text{nonlytic}) \quad (\text{A1})$$

The number of viruses released from lysed cells at time t requires that we multiply $A(x, t)$ by the probability, $h(x)$, that a cell dies within its age class. Viruses that engage the lysing strategy are not associated with a rate like $g(x)$. Rather, they are liberated from the cell, releasing a finite number of virions, $r(x)$. The following summation is obtained:

$$V_L(t) = \sum_{x=0} A(x,t) \cdot h(x) \cdot r(x) \quad (\text{lytic}) \quad (\text{A2})$$

Equations A1 and A2 are added together to give the total number of productive viruses:

$$V(t) = \sum_{x=0} A(x,t) [g(x) + h(x) \cdot r(x)] \quad (\text{A3})$$

For a population of infected cells, the hazard function ensures that we only count dead cells that are lysed within their age class and exclude those that had expired previously (Komarova). Given the cells' lifetime probability distribution, $f(x)$, and their corresponding survivorship, $F^S(x)$, the hazard function is simply the ratio of the two:

$$h(x) = \frac{f(x)}{F^S(x)} \quad (\text{A4})$$

Above, we defined $A(x, t)$ as the number of cells alive at time t within a specific age class, x . The viability of the cell population is a measure of both new viral infections and the cells' ability to overcome the infection. Therefore, $A(x, t)$ is redefined as the number of new infections occurring at a previous time, $t - x$, multiplied by the cell's chance of survival, $F^S(x)$, until time t .

$$A(x,t) = V(t-x) \cdot F^S(x) \quad (\text{A5})$$

Substituting Equations A4 and A5 into Equation A3 we have:

$$V(t) = \sum_{x=0} V(t-x) [F^S(x) \cdot g(x) + f(x) \cdot r(x)] \quad (\text{A6})$$

Dividing both sides by $V(t)$:

$$1 = \sum_{x=0} \frac{V(t-x)}{V(t)} [F^S(x) \cdot g(x) + f(x) \cdot r(x)] \quad (\text{A7})$$

We assume that each age class grows exponentially with time, $V(t) \propto e^{\Gamma t}$, where Γ is the reproductive rate:

$$1 = \sum_{x=0} e^{-\Gamma x} [F^S(x) \cdot g(x) + f(x) \cdot r(x)] \quad (\text{A8})$$

This expression makes sense because more viruses are produced at a later time, thus the ratio of $V(t-x)$ to $V(t)$ will yield negative growth. Allowing the age classes to be subdivided into infinitesimally small categories, the Euler-Lotka equation for virus proliferation is finally obtained:

$$1 = \int_0^{\infty} e^{-\Gamma x} [F^S(x) \cdot g(x) + f(x) \cdot r(x)] dx \quad (\text{A9})$$

Appendix B: Solutions to the Euler-Lotka Equation

The expressions obtained from solving Equations 10 and 11 are found here:

$$\text{Nonlytic: } 1 = c_1 \int_0^{\infty} \theta(x-\lambda) \cdot e^{-\Gamma x} \left[1 + \theta(x-\Delta) e^{-\frac{x-\Delta}{\tau-\Delta}} - \theta(x-\Delta) \right] dx \quad (\text{10})$$

$$1 = \frac{c_1}{\Gamma} e^{-\Gamma \lambda} + \frac{c_1(\tau-\Delta)}{\Gamma(\tau-\Delta)+1} \cdot e^{-\frac{\Gamma(\tau-\Delta) \cdot \max(\lambda, \Delta) + \Delta - \max(\lambda, \Delta)}{\tau-\Delta}} - \frac{c_1}{\Gamma} e^{-\Gamma \cdot \max(\lambda, \Delta)} \quad (\text{B1})$$

$$\text{Lytic: } 1 = \frac{c_2}{\tau-\Delta} \int_0^{\infty} (x-\lambda) \cdot e^{-\Gamma x} \left[\theta(x-\Delta) \cdot e^{-\frac{x-\Delta}{\tau-\Delta}} \right] dx \quad (\text{11})$$

$$1 = \frac{c_2(\lambda\Gamma\Delta - \lambda\Gamma\tau + \Gamma\tau\Delta - \Gamma\Delta^2 + \tau - \lambda)}{(1 + \Gamma\tau - \Gamma\Delta)^2} \cdot e^{-\Gamma\Delta} \quad (\text{B2})$$

Two special cases result from limiting expressions with respect to Δ . Equations B1 and B2 are condensed under these unique circumstances:

$$\text{Special Case I: } \Delta \rightarrow 0, \lambda > \Delta \Rightarrow \begin{cases} \text{Nonlytic: } 1 = \frac{c_1\tau}{\Gamma\tau+1} \cdot e^{-\lambda\left(\frac{\Gamma+1}{\tau}\right)} \\ \text{Lytic: } 1 = \frac{c_2(-\lambda\Gamma\tau + \tau - \lambda)}{(1 + \Gamma\tau)^2} \end{cases} \quad (\text{B3})$$

$$\text{Special Case II: } \Delta \rightarrow \tau, \lambda < \tau \Rightarrow \begin{cases} \text{Nonlytic: } 1 = \frac{c_1}{\Gamma} [e^{-\Gamma\lambda} - e^{-\Gamma\tau}] \\ \text{Lytic: } 1 = c_2(\tau - \lambda) e^{-\Gamma\tau} \end{cases} \quad (\text{B4})$$

Acknowledgements

I would like to express my deepest gratitude and respect towards my faculty mentor, Professor Natalia Komarova.

She was exceptionally patient and gracious throughout my entire research experience. This project is also attributable to the guidance I received from Dr. Bruce Blumberg, Dr. Ingrid Ruf, Dr. Dominik Wodarz, and Said Shokair. Thank you to Professor Bill McClure for his ongoing advice and for encouraging me to pursue mathematics and genetics at UCI. Finally, my sincerest appreciation goes to my parents for their emotional support.

Works Cited

- Abou El Hassan, M., S. Abbas, F. Kruyt and I. van der Meulen-Muileman. "Conditionally Replicating Adenoviruses Kill Tumor Cells via a Basic Apoptotic Machinery-Independent Mechanism That Resembles Necrosis-Like Programmed Cell Death." *Journal of Virology* 78 (2004): 12243-12251.
- Anderson, R., R. May. "The Population Biology of the Interaction Between HIV-1 and HIV-2: Coexistence or Competitive Exclusion?" *AIDS* 10 (1996): 1663-1673.
- Baize, S., S. P. Fisher-Hoch, E. M. Leroy and E. Mavoungou. "Apoptosis in fatal Ebola infection. Does the virus toll the bell for immune system?" *Apoptosis* 5 (2000): 5-7.
- Cann, Alan, J. *Principles of Molecular Biology*. 4th ed. London, UK: Elsevier Academic Press, 2005.
- Carrasco, Luis, Ed. *Mechanisms of Viral Toxicity in Animal Cells*. Boca Raton, Florida: CRC Press, 1987.
- Clever, J., H. Kasamatsu and M. Yamada. "Import of Simian Virus 40 Virions Through Nuclear Pore Complexes (DNA Tumor Virus/Nuclear Transport)." *Proceedings of the National Academy of Sciences* 88 (1991): 7333-7337.
- Cromack, A., J. Blue, and J. Gratzek. "A quantitative ultrastructural study of the development of bluetongue virus in Madin-Darby bovine kidney cells." *Journal of General Virology* 13 (1971): 229-44.
- Kommers, G., C. Brown, D. King and B. Seal. "Virulence of Six Heterogeneous-Origin Newcastle Disease Virus Isolates Before and After Sequential Passages in Domestic Chickens." *Avian Pathology* 32 (2003): 81-93.
- Levin, Bruce R. "The Evolution and Maintenance of Virulence in Microparasites." *Emerging Infectious Diseases* 2 (1996): 93-102.
- Levin, Simon A., Ed. *Population Biology*. Vol. 30. Providence, Rhode Island: American Mathematical Society, 1983.
- Lotka, Alfred J. *Elements of Mathematical Biology*. New York: Dover Publications, Inc., 1956.
- Mangor, J., G. Blissard, M. Johnson and S. Monsma. "A GP64-Null Baculovirus Pseudotyped with Vesicular Stomatitis Virus G Protein." *Journal of Virology* 75 (2001): 2544-2556.
- Mediratta, S. and K. Essani. "The Replication Cycle of Tanapox Virus in Owl Monkey Kidney Cells." *Canadian Journal of Microbiology* 45 (1999): 92-96.
- Morales, Manuel A. "Derivation of Euler." Williams College. 5 June, 2006 <<http://mutualism.williams.edu/BIOLOGY203/Resources/DerivationofEuler.htm>>.
- Murray, Jr., Bertram G. *Population Dynamics, Alternative Models*. New York: Academic Press, 1979.
- Neal, Dick. *Introduction to Population Biology*. Cambridge, United Kingdom: Cambridge University Press, 2004.
- Nowak, M., and R. May. "Superinfection and the Evolution of Parasite Virulence." *Proceedings: Biological Sciences* 255 (1994): 81-89.
- Portner, A., and R. Bussell. "Measles Virus Ribonucleic Acid and Protein Synthesis: Effects of 6-Azauridine and Cycloheximide on Viral Replication." *Journal of Virology* 11 (1973): 46-53.
- Ruf, Ingrid. Personal Communication. 30 June, 2006.
- Voyles, Bruce A. *The Biology of Viruses*. 2nd ed. New York: McGraw Hill, 2002.
- Yamaguchi, T., R. Pollard and Y. Shinagawa. "Relationship Between the Production of Murine Cytomegalovirus and Interferon in Macrophages." *Journal of General Virology* 69 (1988): 2961-2971.
- Yasuda, J., A. Ishihama, M. Nakayama and T. Toyoda. "Regulatory Effects of Matrix Protein Variations on Influenza Virus Growth." *Archives of Virology* 133 (1993): 283-294.